

A SECOND GALAXY MISSING DARK MATTER IN THE NGC 1052 GROUP

PIETER VAN DOKKUM¹, SHANY DANIELI¹, ROBERTO ABRAHAM², CHARLIE CONROY³, AARON J. ROMANOWSKY^{4,5}

Submitted to the Astrophysical Journal Letters

ABSTRACT

The ultra-diffuse galaxy NGC1052-DF2 has a very low velocity dispersion, indicating that it has little or no dark matter. Here we report the discovery of a second galaxy in this class, residing in the same group. NGC1052-DF4 closely resembles NGC1052-DF2 in terms of its size, surface brightness, and morphology; has a similar distance of $D_{\text{sf}} = 19.9 \pm 2.8$ Mpc; and has a similar population of luminous globular clusters extending out to ≥ 7 kpc from the center of the galaxy. Accurate radial velocities of seven clusters were obtained with the Low Resolution Imaging Spectrograph on the Keck I telescope. Their median velocity is $\langle v \rangle = 1445 \text{ km s}^{-1}$, close to the central velocity of 22 galaxies in the NGC1052 group. The rms spread of the observed velocities is very small at $\sigma_{\text{obs}} = 5.8 \text{ km s}^{-1}$. Taking observational uncertainties into account we determine an intrinsic velocity dispersion of $\sigma_{\text{intr}} = 4.2^{+4.4}_{-2.2} \text{ km s}^{-1}$, consistent with the expected value from the stars alone ($\sigma_{\text{stars}} \approx 7 \text{ km s}^{-1}$) and lower than expected from a standard NFW halo ($\sigma_{\text{halo}} \sim 30 \text{ km s}^{-1}$). We conclude that NGC1052-DF2 is not an isolated case but that a class of such objects exists. The origin of these large, faint galaxies with an excess of luminous globular clusters and an apparent lack of dark matter is, at present, not understood.

Keywords: galaxies: evolution — galaxies: structure

1. INTRODUCTION

Sensitive surveys using state of the art telescopes have identified large numbers of intrinsically-large galaxies with very low surface brightness (e.g., van Dokkum et al. 2015; Koda et al. 2015; van der Burg, Muzzin, & Hoekstra 2016). These “ultra diffuse galaxies” (UDGs), with sizes $R_e > 1.5$ kpc and central surface brightness $\mu_g > 24 \text{ mag arcsec}^{-2}$, have been found in many different environments (including the Local Group; Martin et al. 2016; Torrealba et al. 2018), and have a wide range of properties (see, e.g., Merritt et al. 2016).

One of the most intriguing UDGs that have been studied so far is NGC1052-DF2 in the NGC 1052 group. Using a combination of Hubble Space Telescope *HST* Advanced Camera for Surveys (ACS) imaging and Keck spectroscopy, we determined that this galaxy has an unusual population of luminous globular cluster-like objects (van Dokkum et al. 2018c). Furthermore, from the radial velocities of ten of these globular clusters we determined that the galaxy appears to have little or no dark matter ($\lesssim 10^8 M_\odot$; van Dokkum et al. 2018b; Wasserman et al. 2018; Danieli et al. 2019). Both aspects are surprising: the globular cluster luminosity function was thought to be universal (Rejkuba 2012), and a galaxy with a stellar mass of $\sim 2 \times 10^8 M_\odot$ should have a dark matter mass of $\sim 6 \times 10^{10} M_\odot$ (Behroozi, Wechsler, & Conroy 2013b).

Although these unexpected results were initially greeted with some skepticism (e.g., Martin et al. 2018; Laporte, Agnello, & Navarro 2018; Nusser 2018; Hayashi & Inoue 2018; Ogiya 2018; Trujillo et al. 2019), recent studies have con-

firmed the unusual nature of NGC1052-DF2: the distance to the galaxy ($D \approx 20$ kpc) was placed on surer footing (van Dokkum et al. 2018a; Blakeslee & Cantiello 2018) and, crucially, Danieli et al. (2019) confirmed the low mass of NGC1052-DF2 by measuring the stellar velocity dispersion of the galaxy to be $\sigma_{\text{stars}} = 8.4 \pm 2.1 \text{ km s}^{-1}$ (we note that a competing claim is made in Emsellem et al. 2019, based on data of much lower spectral resolution).

With this confirmation, the central unanswered question is whether NGC1052-DF2 is an isolated case or representative of a population of similar galaxies. This is important for judging the likelihood of interpretations that require unusual orbits or viewing angles (see, e.g., Ogiya 2018) and, most importantly, for judging the relevance of NGC1052-DF2 for our ideas about galaxy formation and the relation between dark matter and normal matter. With the important exception of tidal dwarfs (Bournaud et al. 2007; Gentile et al. 2007; Lelli et al. 2015), it is thought that a gravitationally-dominant dark matter halo is the *sine qua non* for the formation of a galaxy. If galaxies such as NGC1052-DF2 are fairly common we may have to revise our concept of what a galaxy *is*, and come up with alternative pathways for creating galaxy-mass stellar systems.

Here we report the discovery of a galaxy that shares essentially all of NGC1052-DF2’s unusual properties, to a remarkable degree. It is in the same group, has a similar size, luminosity, and color, the same morphology, the same population of luminous globular clusters, and the same extremely low velocity dispersion.

2. NGC1052-DF4

NGC1052-DF4 is a low surface brightness galaxy in the field of the elliptical galaxy NGC 1052. It is part of a sample of 23 objects that we identified in images taken with the Dragonfly Telephoto Array (Abraham & van Dokkum 2014) and followed up with the ACS on *HST* (see Cohen et al. 2018). Unlike NGC1052-DF2, which had been described earlier by Fosbury et al. (1978) and Karachentsev et al. (2000),

¹ Astronomy Department, Yale University, 52 Hillhouse Ave, New Haven, CT 06511, USA

² Department of Astronomy & Astrophysics, University of Toronto, 50 St. George Street, Toronto, ON M5S 3H4, Canada

³ Harvard-Smithsonian Center for Astrophysics, 60 Garden Street, Cambridge, MA, USA

⁴ Department of Physics and Astronomy, San José State University, San Jose, CA 95192, USA

⁵ University of California Observatories, 1156 High Street, Santa Cruz, CA 95064, USA

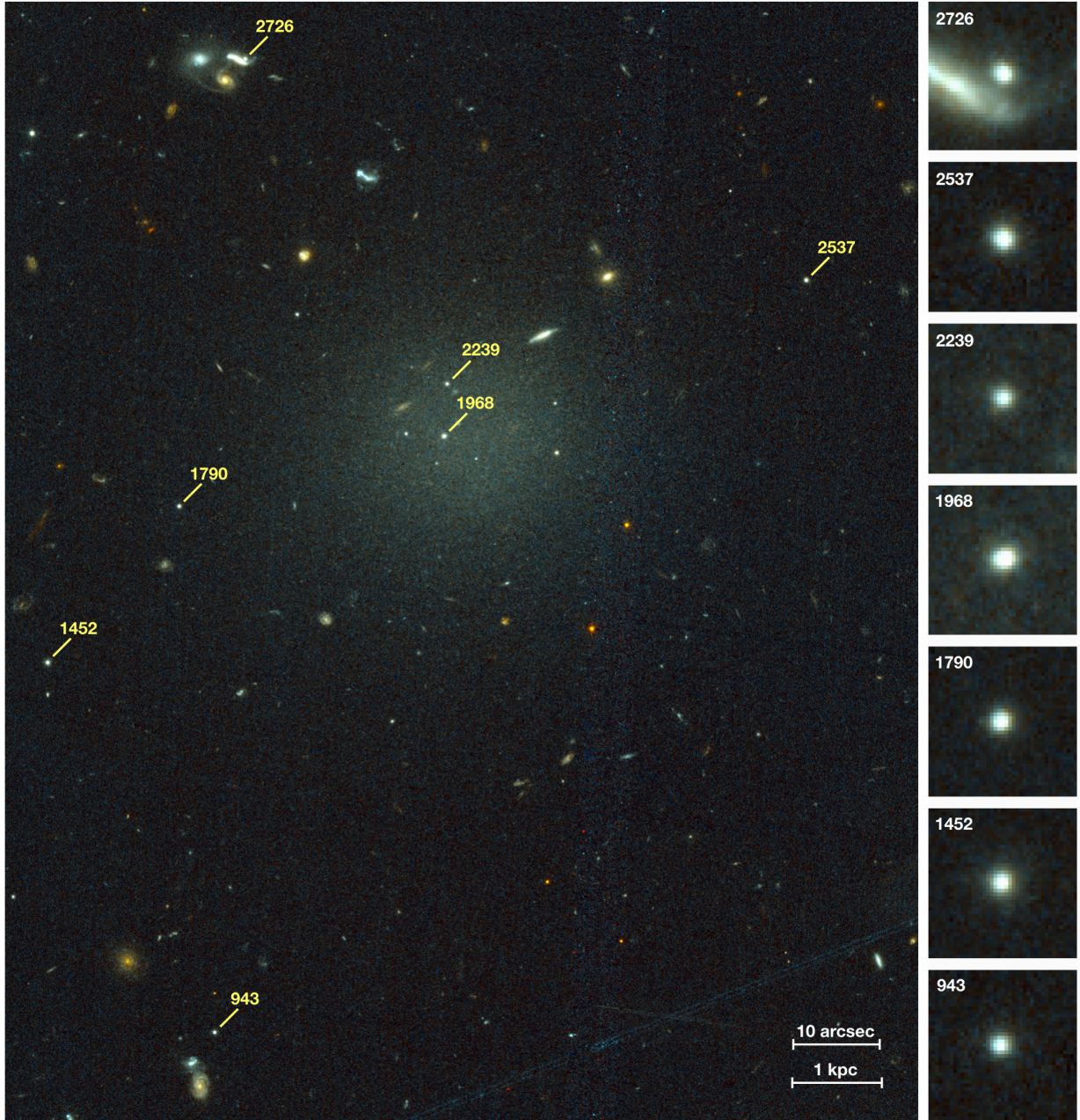


Figure 1. *HST* ACS image of NGC1052-DF4, created from the V_{606} and I_{814} bands. The galaxy has a smooth, spheroidal morphology with a low Sérsic index ($n = 0.79$). The highlighted objects are spectroscopically-confirmed globular clusters.

NGC1052-DF4 was discovered with Dragonfly.⁶ The *HST* image is shown in Fig. 1.

Basic parameters, as derived from the *HST* imaging, are given in Cohen et al. (2018). Its surface brightness fluctuation distance is $D_{\text{sbf}} = 19.9 \pm 2.8$ Mpc, and as highlighted in Fig. 5 of van Dokkum et al. (2018a) its color-magnitude diagram is very similar to that of NGC1052-DF2. We infer that the galaxy is part of the NGC 1052 group, and use $D = 20$ Mpc for distance-dependent quantities. The galaxy is well-fitted by a 2D Sérsic (1968) profile with a Sérsic index of $n = 0.79$, an axis ratio of $b/a = 0.89$, central surface

brightness $\mu(V_{606}, 0) = 23.7$, and major axis half-light radius $R_e = 1.6$ kpc. These properties place the galaxy just inside the UDG selection box (see Fig. 10 of Cohen et al. 2018). The total absolute magnitude is $M_{V,606} = -15.0 \pm 0.1$, corresponding to $L_{V,606} = (7.7 \pm 0.8) \times 10^7 L_\odot$. Assuming $(M/L)_{\text{stars},V} = (2.0 \pm 0.5) M_\odot/L_\odot$ (see van Dokkum et al. 2018b) the implied total stellar mass is $M_{\text{stars}} = (1.5 \pm 0.4) \times 10^8 M_\odot$.

At first glance NGC1052-DF4 seemed to lack the spectacular population of bright globular cluster-like objects that initially drew our attention to NGC1052-DF2 (see van Dokkum et al. 2018b, 2018c). However, careful inspection of the *HST* imaging data shows that the NGC1052-DF4 field actually *does* contain objects with similar sizes, colors, and apparent magnitudes as the globular clusters in NGC1052-DF2 –

⁶ This is a somewhat academic point as the galaxy is not particularly faint; it is clearly visible in Plate 1 of Fosbury et al. (1978) and in many other imaging datasets.

Table 1
NGC1052-DF4 Globular Clusters

Id	RA (J2000)	Dec (J2000)	R^a [kpc] ^b	$M_{V,606}$ [mag] ^b	v [km s ⁻¹]
DF4	2 ^h 39 ^m 15.11 ^s	-8°6′58″.6	...	-15.0	...
2726	2 ^h 39 ^m 16.75 ^s	-8°6′16″.7	4.69	-9.2	1441.2 ^{+4.9} _{-4.8}
2537	2 ^h 39 ^m 12.53 ^s	-8°6′41″.4	4.08	-9.2	1451.0 ^{+3.6} _{-3.3}
2239	2 ^h 39 ^m 15.23 ^s	-8°6′53″.0	0.57	-8.6	1457.1 ^{+4.6} _{-4.6}
1968	2 ^h 39 ^m 15.25 ^s	-8°6′58″.8	0.20	-9.8	1445.4 ^{+2.6} _{-2.3}
1790	2 ^h 39 ^m 17.24 ^s	-8°7′06″.7	3.17	-9.0	1438.4 ^{+4.8} _{-4.6}
1452	2 ^h 39 ^m 18.23 ^s	-8°7′24″.1	5.13	-9.1	1445.5 ^{+4.1} _{-4.1}
943	2 ^h 39 ^m 13.46 ^s	-8°6′37″.1	7.01	-8.6	1445.1 ^{+5.0} _{-5.2}

^a Distance from the center of the galaxy.

^b For an assumed distance of $D = 20$ Mpc.

but that they are even more spread out relative to the body of the galaxy. This unexpected finding inspired us to obtain spectra of these candidate globular clusters, to determine whether they are actually in a single structure and, if so, to use them to constrain the mass of NGC1052-DF4.

3. SPECTROSCOPY

We observed compact objects in the NGC1052-DF4 field with the dual arm Low Resolution Imaging Spectrograph (LRIS) on the Keck I telescope. The sample selection is modeled upon the properties of the confirmed clusters in NGC1052-DF2. We used SExtractor (Bertin & Arnouts 1996) to measure total magnitudes, colors, and FWHM sizes of objects in the *HST* images, following the methodology outlined in van Dokkum et al. (2018c). Priority was given to objects with $I_{814} < 23$, $0.20 < V_{606} - I_{814} < 0.43$, and $0''.12 < \text{FWHM} < 0''.30$, as all 11 clusters from van Dokkum et al. (2018c) satisfy these criteria. In NGC1052-DF4, seven objects fall within these limits. They have a mean total magnitude of $\langle I_{814} \rangle = 22.10$ with a 1σ rms spread of 0.39 mag. Objects just outside these selection limits were given lower priority.

All seven high priority objects could be fitted in a single multi-slit mask, along with several lower priority targets. This mask was observed on November 6 2018 for a total of 19,800 s, split over eleven 1,800 s exposures. Conditions were excellent. On the blue side the low resolution 300 lines mm⁻¹ grism blazed at 5000 Å was used, and on the red side the 1200 lines mm⁻¹ grating blazed at 9000 Å. Here only the high resolution red-side observations are discussed. The slit width of the mask is 0''.8, providing a resolution of $\sigma_{\text{instr}} \approx 25$ km s⁻¹ near the Calcium triplet.

The data reduction follows the same procedures as those outlined in van Dokkum et al. (2018b). Briefly, the slit edges and the sky lines are used to correct the spectra for distortions. The sky line modeling and subtraction is done using the method of Kelson (2003), which minimizes interpolation-related residuals. The sky lines are also used for wavelength calibration. Each individual 1,800 s exposure is analyzed independently to limit the effects of flexure on the distortion modeling and wavelength calibration. The exposures are combined using optimal weighting, and 1D spectra are extracted by weighting each line in the 2D spectrum by the S/N

⁷ There are three objects with $23.0 < I_{814} < 23.5$ that satisfy the color and size criteria.

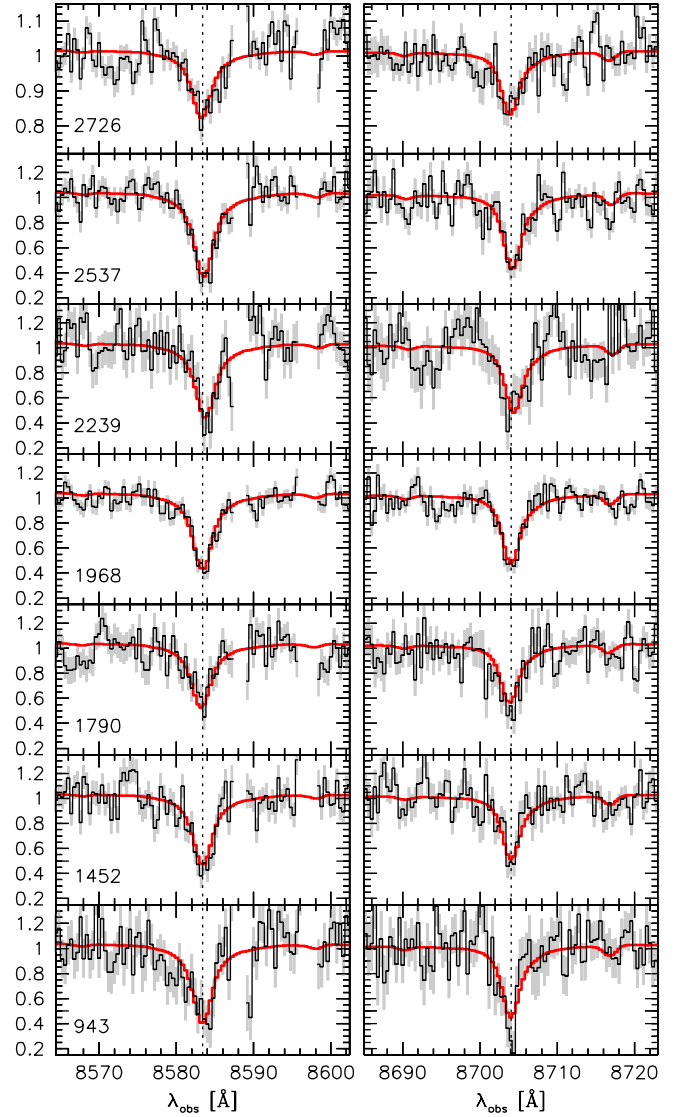


Figure 2. Keck/LRIS spectra of the seven globular cluster-like objects in the region of the strongest Ca triplet lines, with the uncertainties shown in grey. The model spectra that were fitted to the data to determine radial velocities are shown in red. The vertical dashed line indicates the median velocity of $\langle v \rangle = 1445$ km s⁻¹.

ratio.

An inspection of the spectra shows that all seven bright globular cluster candidates indeed have strong absorption features at the approximate redshift of the NGC 1052 group. Two other objects (which do not satisfy the strict color and size criteria) turn out to be compact background galaxies, and the rest of the lower priority objects are too faint for a redshift measurement. We show the spectra of the seven high priority targets in Fig. 2, focusing on the regions near the redshifted $\lambda\lambda 8542.09, 8662.14$ Å lines of the Ca triplet.⁸ The weaker $\lambda 8498.02$ Å line is mostly masked, as it coincides with a strong sky line at the redshift of NGC1052-DF4. Despite a shorter total integration time the spectra are of higher quality than those of most of the clusters in NGC1052-DF2 (van Dokkum et al. 2018b), due to better seeing and photomet-

⁸ Note that the spectrum of GC-2726 is blended with a star forming background galaxy.

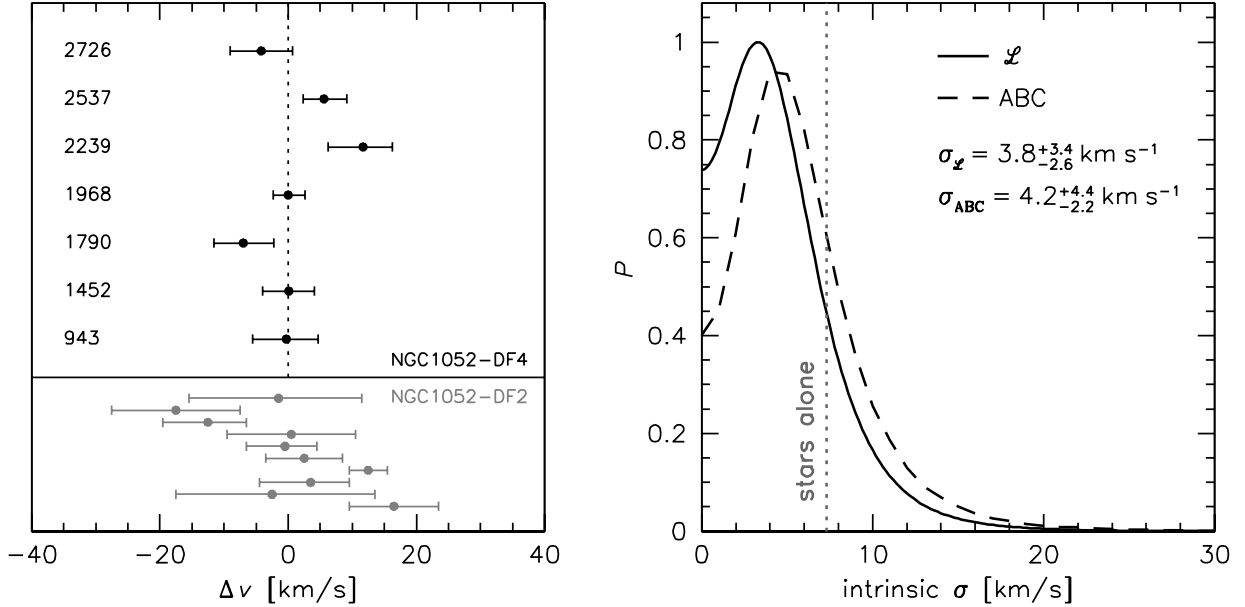


Figure 3. *Left panel:* Graphical representation of the globular cluster velocities in NGC1052-DF4 (top) and NGC1052-DF2 (bottom), relative to the median. *Right panel:* Constraints on the intrinsic velocity dispersion of NGC1052-DF4 from the seven clusters, using the likelihood estimator (solid) and approximate bayesian computation (dashed). The expected velocity dispersion for a normal dark matter halo is $\sim 30 \text{ km s}^{-1}$. The expected dispersion from the stellar mass alone, with no dark matter, is $\approx 7 \text{ km s}^{-1}$ (vertical broken line).

ric conditions during the observations. The median S/N ratio near the Ca triplet is 17 Å^{-1} .

4. KINEMATICS

4.1. Radial Velocities

Radial velocities of the seven clusters are determined by fitting the data with a synthetic 11 Gyr, $[\text{Fe}/\text{H}]=-1$ stellar population synthesis model (Conroy, Gunn, & White 2009; Choi et al. 2016), convolved to the instrumental resolution. The fit is performed in the redshifted Calcium triplet region $8520 \text{ Å} < \lambda < 8740 \text{ Å}$, using the `emcee` MCMC algorithm (Foreman-Mackey et al. 2013). The fit is regularized by dividing the data and template by a polynomial of order $100^{-1} \Delta \lambda [\text{Å}]$. Two free parameters are fitted: the velocity and an additive continuum offset, to account for any template mismatch. With the exception of the blended spectrum of GC-2726 this parameter is typically close to zero. Errors are determined from simulations. In each simulation the residuals of the fits are randomly shuffled and the velocity fit is repeated. Residuals from sky lines are shuffled separately from the rest of the spectrum. The width of the distribution of the resulting velocities is taken as the uncertainty in the fit (see van Dokkum et al. 2018b). The results are not sensitive to the details of these procedures; owing to the high S/N ratio of the spectra the velocities and the associated uncertainties are very stable.

The velocities are listed in Table 1 and displayed in the left panel of Fig. 3. The random uncertainties are small; the mean $\pm 1\sigma$ error is $\pm 4 \text{ km s}^{-1}$. The median (mean) velocity is $\langle v \rangle = 1445 \text{ km s}^{-1}$ (1446 km s^{-1}). This is very close to the average velocity of other galaxies in the NGC 1052 group. Including NGC1052-DF2 there are 22 galaxies in the NASA Extragalactic Database within a radius of two degrees centered on NGC 1052 in the velocity range $0 < v < 2500 \text{ km s}^{-1}$. All are in the range $1241 \text{ km s}^{-1} < v < 1803 \text{ km s}^{-1}$, with a bi-weight mean of $v_{\text{group}} = 1438 \pm 25 \text{ km s}^{-1}$ and width $\sigma_{\text{group}} =$

$128 \pm 19 \text{ km s}^{-1}$.

4.2. Velocity Dispersion

The velocity range of the seven clusters is extremely small, echoing our earlier result for NGC1052-DF2. The observed rms, before correcting for observational uncertainties, is only 5.8 km s^{-1} (compared to 10 km s^{-1} for NGC1052-DF2). We use two methods to determine the intrinsic dispersion σ_{intr} and its associated uncertainties. Both methods use a generative model whose parameters are constrained by assessing the probability of measuring the observed velocity distribution. The model is a simple Gaussian with the center and width as free parameters. The classical method, used extensively for determining the kinematics of dwarf galaxies in the Local Group from the velocities of individual stars (e.g., Simon & Geha 2007; Martin et al. 2007), is to construct the likelihood function:

$$\mathcal{L} = \prod_{i=1}^{i \leq 7} \frac{1}{\sqrt{2\pi}\sigma_{\text{eff}}} \exp \left[-0.5 \left(\frac{v_i - \mu}{\sigma_{\text{eff}}} \right)^2 \right], \quad (1)$$

with v_i the velocities of the individual tracers, μ the mean of the model, and $\sigma_{\text{eff}}^2 = \sigma_{\text{intr}}^2 + e_i^2$ with σ_{intr} the model dispersion and e_i the uncertainty in velocity v_i (calculated by averaging the positive and negative error bars). The likelihood, marginalized over μ , is shown by the solid line in the right panel of Fig. 3. The likelihood analysis gives $\sigma_{\text{intr}} = 3.8^{+3.4}_{-2.6} \text{ km s}^{-1}$, where the uncertainties contain 68 % of the probability. The 90 % (95 %) confidence level upper limit is 8.6 km s^{-1} (10.4 km s^{-1}).

The second method is approximate Bayesian computation (ABC; Tavare et al. 1997), which approximates the posterior distribution with simulations. For each set of model parameters ($\mu, \sigma_{\text{intr}}$) a large number of simulated datasets $\hat{D} = (\hat{v}_1, \hat{v}_2, \dots, \hat{v}_7)$ are created by randomly drawing velocities from the model and linearly perturbing these values with

errors that are themselves randomly drawn from Gaussians of width (e_1, e_2, \dots, e_7) . These N datasets are compared to the actual data D through a summary statistic S . Simulations that satisfy the criterion

$$\delta(S(\hat{D}), S(D)) < e \quad (2)$$

are retained, with δ the absolute distance between the summary statistics and e a small positive number. For a given choice of $(\mu, \sigma_{\text{intr}})$ the posterior is proportional to the number of simulations that are retained. ABC does not assume a functional form of the likelihood, and summary statistics can be chosen that are best suited to particular situations (see, e.g., van Dokkum et al. 2018b). Another advantage is that it does not suffer from the “small sample bias” discussed in Laporte et al. (2018). We calculate the ABC posterior using $N = 10^4$, $e = 0.1$, and the rms as the summary statistic (Fig. 3). ABC gives a similar result as the likelihood: $\sigma_{\text{intr}} = 4.2^{+4.4}_{-2.2} \text{ km s}^{-1}$. The small difference may reflect the likelihood’s sensitivity to small sample bias (see Laporte et al. 2018).

4.3. Implied Mass

Quantitative constraints on the halo mass are highly uncertain with seven tracers and require extensive modeling (see, e.g., Laporte et al. 2018; Wasserman et al. 2018). Here we simply test the hypothesis that there is no dark matter halo and all the mass is in the form of stars. Following Beasley et al. (2016) and van Dokkum et al. (2018b) we estimate the mass within the outermost globular cluster using the tracer mass estimator (TME) method of Watkins, Evans, & An (2010):

$$M_{\text{TME}} = \frac{C}{G} \langle (\Delta v')^2 r^\alpha \rangle r_{\text{out}}^{1-\alpha}. \quad (3)$$

Here $\Delta v' = f^{-1}(v - 1445.7)$ are the velocities of the individual tracers, with $f = \sigma_{\text{obs}}/\sigma_{\text{intr}} = 1.4^{+1.5}_{-0.7}$. The parameter α is the slope of the potential and C is a constant given by

$$C = \frac{4\Gamma(\frac{\alpha}{2} + \frac{5}{2})}{\sqrt{\pi}\Gamma(\frac{\alpha}{2} + 1)} \frac{\alpha + \gamma - 2\beta}{\alpha + 3 - \beta(\alpha + 2)}, \quad (4)$$

with γ the power-law slope of the 3D density profile of the tracers and $\beta = 1 - \sigma_t^2/\sigma_r^2$ the Binney anisotropy parameter. For simplicity we assume that $\beta = 0$ and that the globular clusters trace the potential,⁹ so that $\gamma = \alpha + 2$. If all the mass is in stars the potential is similar to that of a point mass for most of the globular clusters, and $\alpha \approx 1$.

With these assumptions we find an enclosed mass within 7 kpc of $M_{\text{TME}} = 0.4^{+1.2}_{-0.3} \times 10^8 M_\odot$. The total stellar mass is $M_{\text{stars}} = (1.5 \pm 0.4) \times 10^8 M_\odot$ (see § 2), and we conclude that we cannot reject the hypothesis that there is no dark matter in this system. Another way to phrase this is that the intrinsic dispersion of $\sigma_{\text{intr}} = 4.2^{+4.4}_{-2.2} \text{ km s}^{-1}$ is consistent with that expected from the stars alone ($\sigma_{\text{stars}} \approx 7.3 \pm 1.9 \text{ km s}^{-1}$; Wolf et al. 2010). For reference, the expected dispersion from an NFW halo of the expected mass is $\sigma_{\text{halo}} \approx 30 \text{ km s}^{-1}$ (Łokas & Mamon 2001; Behroozi et al. 2013a).

5. DISCUSSION

In this *Letter* we have presented a doppelgänger of the dark matter-deficient galaxy NGC1052-DF2. NGC1052-DF4 is in

the same group as NGC1052-DF2 and has a similar size, luminosity, morphology, globular cluster population, and velocity dispersion. The immediate implication is that NGC1052-DF2 is not an isolated case but that a class of such galaxies exists, and given how little we know about galaxies in the UDG parameter space it may well be that they are fairly common.

The discovery of NGC1052-DF4 does not bring us much closer to understanding how such galaxies are formed, although it does effectively rule out “tail of the distribution” explanations for NGC1052-DF2. Suggestions that the true velocity dispersion is in the upper 10 % of the posterior distribution (Martin et al. 2018), that the galaxy could be an asymmetric thin disk seen exactly face-on (see van Dokkum et al. 2018b), is on a precisely-tuned orbit (Ogiya 2018), or that it was formed in a carefully orchestrated sequence of events (e.g., Fensch et al. 2019), are far less likely now that there is a second system.

One pathway for creating dark matter-deficient galaxies is by forming them out of gas that was expelled from a disk with a high baryon fraction, through a tidal interaction (e.g., Duc & Mirabel 1998; Gentile et al. 2007). However, NGC1052-DF2 and NGC1052-DF4 lack two of the key identifying features of such objects. First, as the gas must have originated in a dense disk to explain the low dark matter fraction, it should be pre-enriched. Therefore, tidal dwarfs should have a high metallicity for their mass (Duc & Mirabel 1998), and this is not the case for NGC1052-DF2 (van Dokkum et al. 2018c; Fensch et al. 2019). Second, although we identify several tidal features associated with NGC 1052 in the Dragonfly imaging, there is no evidence for debris in the vicinity of NGC1052-DF2 or NGC1052-DF4, although this has been reported around other old tidal dwarfs (see Duc et al. 2014).

More broadly, the environment of NGC1052-DF4 does not shed much light on its origins. The galaxy is highlighted in a wide field of view in Fig. 4. As noted in § 4.1 the systemic velocity of NGC1052-DF4 is almost identical to the average of the NGC 1052 group galaxies. It is at a projected distance of 28.5 (165 kpc) from NGC 1052 itself, a factor of two further than NGC1052-DF2. It is close (23 kpc) in projection to NGC 1035, which has a radial velocity of $cz = 1241 \text{ km s}^{-1}$. Given their velocity difference of 204 km s^{-1} it is unlikely that NGC1052-DF4 is a satellite of this low mass disk galaxy (Truong et al. 2017). Apart from the relatively large systemic velocity of NGC1052-DF2 (1803 km s^{-1} ; Danieli et al. 2019) there is nothing obviously “special” about the two galaxies in relation to other group members, or about the NGC 1052 group when compared to other structures.

Although it is hazardous to draw conclusions from such correlations, it seems likely that the low dark matter mass in these galaxies is somehow related to their unprecedented globular cluster systems (see van Dokkum et al. 2018c). The combined number of confirmed clusters with $M_V < -8.5$ in NGC1052-DF2 and NGC1052-DF4 is nearly the same as the number of globular clusters in the Milky Way to that limit (18 versus 23), despite the factor of 100 difference in stellar mass between them. The seven confirmed clusters in NGC1052-DF4 make up 3 % of its total luminosity, and the two most distant clusters by themselves make up ≈ 70 % of NGC1052-DF4’s luminosity at $R > 5 \text{ kpc}$. The properties of the NGC1052-DF4 globular clusters will be the topic of a future paper. Here we only note that their median size is $\langle r_h \rangle = 4.1 \text{ pc}$, similar to that of Milky Way clusters in the same luminosity range (Harris 1996; Harris, Harris, & Alessi 2013).

⁹ In reality the globular clusters likely follow a shallower profile; the TME mass is even lower for lower values of γ .

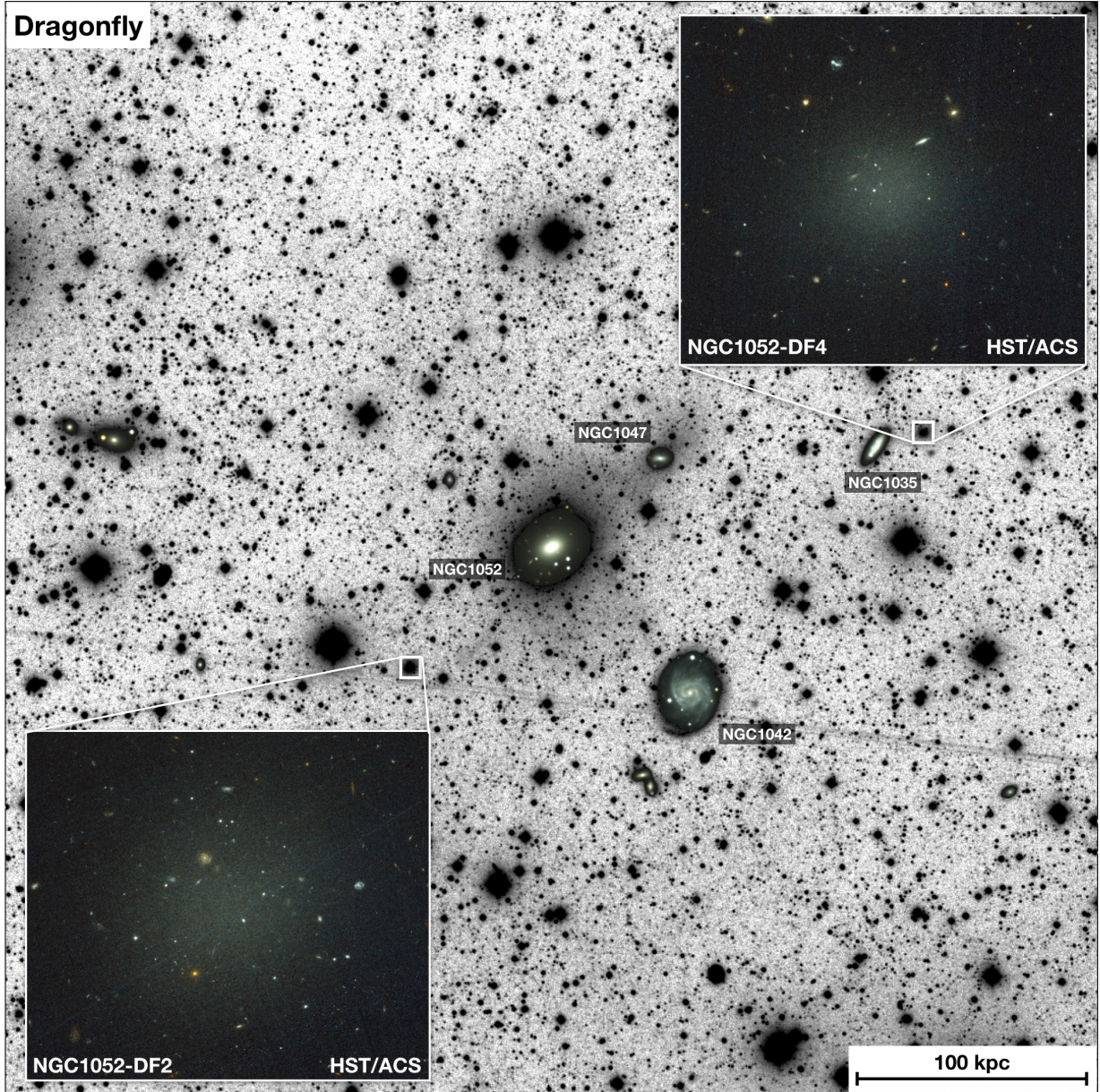


Figure 4. Central area of the summed $g+r$ Dragonfly image of the NGC 1052 field. The displayed area covers $1.33^\circ \times 1.33^\circ$, corresponding to $466 \text{ kpc} \times 466 \text{ kpc}$ for a distance of 20 Mpc. NGC1052-DF2 and NGC1052-DF4 are highlighted. The *HST* images span $93'' \times 80''$ ($9.0 \text{ kpc} \times 7.6 \text{ kpc}$). We find several distinct tidal features associated with NGC 1052, including clear evidence for an interaction with NGC 1047. No tidal debris is detected near NGC1052-DF2 or NGC1052-DF4.

Looking ahead, we can determine the stellar velocity dispersion of NGC1052-DF4 (see Emsellem et al. 2019; Danieli et al. 2019), constrain its dark matter mass (e.g., Laporte et al. 2018; Wasserman et al. 2018), and assess the implications for alternative gravity (van Dokkum et al. 2018b; Famaey, McGaugh, & Milgrom 2018): taken together, NGC1052-DF2 and NGC1052-DF4 seem in tension with recent predictions from Modified Newtonian Dynamics (Müller, Famaey, & Zhao 2019). Given the adagium “one is an exception and two is a population” this new object provides impetus for charac-

terizing the properties of diffuse, dark matter-deficient galaxies as a class. We are performing wide field surveys with the Dragonfly Telephoto Array to identify other candidates.

Support from STScI grants HST-GO-13682 and HST-GO-14644, as well as NSF grants AST-1312376, AST-1613582, and AST-1515084 is gratefully acknowledged. AJR is a Research Corporation for Science Advancement Cottrell Scholar.

REFERENCES

- Abraham, R. G. & van Dokkum, P. G. 2014, *PASP*, 126, 55
 Beasley, M. A., Romanowsky, A. J., Pota, V., Navarro, I. M., Martinez Delgado, D., Neyer, F., & Deich, A. L. 2016, *ApJL*, 819, L20
 Behroozi, P. S., Marchesini, D., Wechsler, R. H., Muzzin, A., Papovich, C., & Stefanon, M. 2013a, *ApJL*, 777, L10
 Behroozi, P. S., Wechsler, R. H., & Conroy, C. 2013b, *ApJ*, 770, 57
 Bertin, E. & Arnouts, S. 1996, *A&AS*, 117, 393

- Blakeslee, J. P. & Cantiello, M. 2018, *Research Notes of the American Astronomical Society*, 2, 146
- Bournaud, F., Duc, P.-A., Brinks, E., Boquien, M., Amram, P., Lisenfeld, U., Koribalski, B. S., Walter, F., et al. 2007, *Science*, 316, 1166
- Choi, J., Dotter, A., Conroy, C., Cantiello, M., Paxton, B., & Johnson, B. D. 2016, *ApJ*, 823, 102
- Cohen, Y., van Dokkum, P., Danieli, S., Romanowsky, A. J., Abraham, R., Merritt, A., Zhang, J., Mowla, L., et al. 2018, *ApJ*, 868, 96
- Conroy, C., Gunn, J. E., & White, M. 2009, *ApJ*, 699, 486
- Danieli, S., van Dokkum, P., Conroy, C., Abraham, R., & Romanowsky, A. J. 2019, *ApJ Letters*, submitted (arXiv:1901.03711)
- Duc, P.-A. & Mirabel, I. F. 1998, *A&A*, 333, 813
- Duc, P.-A., Paudel, S., McDermid, R. M., Cuillandre, J.-C., Serra, P., Bournaud, F., Cappellari, M., & Emsellem, E. 2014, *MNRAS*, 440, 1458
- Emsellem, E., van der Burg, R. F. J., Fensch, J., Jerabkova, T., Zanella, A., Agnello, A., Hilker, M., Mueller, O., et al. 2018, *A&A*, submitted (arXiv:1812.07345)
- Famaey, B., McGaugh, S., & Milgrom, M. 2018, *MNRAS*, 480, 473
- Fensch, J., van der Burg, R. F. J., Jerabkova, T., Emsellem, E., Zanella, A., Agnello, A., Hilker, M., Mueller, O., et al. 2018, *A&A*, submitted (arXiv:1812.07346)
- Foreman-Mackey, D., Hogg, D. W., Lang, D., & Goodman, J. 2013, *PASP*, 125, 306
- Fosbury, R. A. E., Mebold, U., Goss, W. M., & Dopita, M. A. 1978, *MNRAS*, 183, 549
- Gentile, G., Famaey, B., Combes, F., Kroupa, P., Zhao, H. S., & Tiret, O. 2007, *A&A*, 472, L25
- Harris, W. E. 1996, *AJ*, 112, 1487
- Harris, W. E., Harris, G. L. H., & Alessi, M. 2013, *ApJ*, 772, 82
- Hayashi, K. & Inoue, S. 2018, *MNRAS*, 481, L59
- Karachentsev, I. D., Karachentseva, V. E., Suchkov, A. A., & Grebel, E. K. 2000, *A&AS*, 145, 415
- Kelson, D. D. 2003, *PASP*, 115, 688
- Koda, J., Yagi, M., Yamanoi, H., & Komiyama, Y. 2015, *ApJL*, 807, L2
- Laporte, C. F. P., Agnello, A., & Navarro, J. F. 2018, *MNRAS*
- Lelli, F., Duc, P.-A., Brinks, E., Bournaud, F., McGaugh, S. S., Lisenfeld, U., Weilbacher, P. M., Boquien, M., et al. 2015, *A&A*, 584, A113
- Lokas, E. L. & Mamon, G. A. 2001, *MNRAS*, 321, 155
- Martin, N. F., Collins, M. L. M., Longeard, N., & Tollerud, E. 2018, *ApJL*, 859, L5
- Martin, N. F., Ibata, R. A., Chapman, S. C., Irwin, M., & Lewis, G. F. 2007, *MNRAS*, 380, 281
- Martin, N. F., Ibata, R. A., Lewis, G. F., McConnachie, A., Babul, A., Bate, N. F., Bernard, E., Chapman, S. C., et al. 2016, *ApJ*, 833, 167
- Merritt, A., van Dokkum, P., Danieli, S., Abraham, R., Zhang, J., Karachentsev, I. D., & Makarova, L. N. 2016, *ApJ*, 833, 168
- Müller, O., Famaey, B., & Zhao, H. 2019, *A&A*, in press (arXiv:1901.02679)
- Nusser, A. 2018, *ApJ*, 863, L17
- Ogiya, G. 2018, *MNRAS*, 480, L106
- Rejkuba, M. 2012, *Ap&SS*, 341, 195
- Sersic, J. L. 1968, *Atlas de galaxias australes* (Cordoba, Argentina: Observatorio Astronomico, 1968)
- Simon, J. D. & Geha, M. 2007, *ApJ*, 670, 313
- Tavare, S., Balding, D. J., Griffiths, R. C., & Donnelly, P. 1997, *Genetics*, 145, 505
- Torrealba, G., Belokurov, V., Koposov, S. E., Li, T. S., Walker, M. G., Sanders, J. L., Geringer-Sameth, A., Zucker, D. B., et al. 2019, *MNRAS*, submitted (arXiv:1811.04082)
- Trujillo, I., Beasley, M. A., Borlaff, A., Carrasco, E. R., Di Cintio, A., Filho, M., Monelli, M., Montes, M., et al. 2019, *MNRAS*, submitted (arXiv:1806.10141)
- Truong, P. N., Newman, A. B., Simon, J. D., Blitz, L., Ellis, R., & Bolatto, A. 2017, *ApJ*, 843, 37
- van der Burg, R. F. J., Muzzin, A., & Hoekstra, H. 2016, *A&A*, 590, A20
- van Dokkum, P., Danieli, S., Cohen, Y., Romanowsky, A. J., & Conroy, C. 2018a, *ApJL*, 864, L18
- van Dokkum, P., Danieli, S., Cohen, Y., Merritt, A., Romanowsky, A. J., Abraham, R., Brodie, J., Conroy, C., et al. 2018b, *Nature*, 555, 629
- van Dokkum, P., Cohen, Y., Danieli, S., Kruijssen, J. M. D., Romanowsky, A. J., Merritt, A., Abraham, R., Brodie, J., et al. 2018c, *ApJL*, 856, L30
- van Dokkum, P. G., Abraham, R., Merritt, A., Zhang, J., Geha, M., & Conroy, C. 2015, *ApJL*, 798, L45
- Wasserman, A., Romanowsky, A. J., Brodie, J., van Dokkum, P., Conroy, C., Abraham, R., Cohen, Y., & Danieli, S. 2018, *ApJL*, 863, L15
- Watkins, L. L., Evans, N. W., & An, J. H. 2010, *MNRAS*, 406, 264
- Wolf, J., Martinez, G. D., Bullock, J. S., Kaplinghat, M., Geha, M., Muñoz, R. R., Simon, J. D., & Avedo, F. F. 2010, *MNRAS*, 406, 1220